

# Quantum phase transitions in superconducting arrays under external magnetic fields

Beom Jun Kim<sup>1,\*</sup>, Gun Sang Jeon<sup>1</sup>, M.-S. Choi<sup>2</sup>, and M.Y. Choi<sup>1</sup>

<sup>1</sup>*Department of Physics and Center for Theoretical Physics  
Seoul National University, Seoul 151-742, Korea*

<sup>2</sup>*Department of Physics and Pohang Superconductivity Center  
Pohang University of Science and Technology, Pohang 790-784, Korea*

We study the zero-temperature phase transitions of two-dimensional superconducting arrays with both the self- and the junction capacitances in the presence of external magnetic fields. We consider two kinds of excitations from the Mott insulating phase: charge-dipole excitations and single-charge excitations, and apply the second-order perturbation theory to find their energies. The resulting phase boundaries are found to depend strongly on the magnetic frustration, which measures the commensurate-incommensurate effects. Comparison of the obtained values with those in recent experiment suggests the possibility that the superconductor-insulator transition observed in experiment may not be of the Berezinskii-Kosterlitz-Thouless type. The system is also transformed to a classical three-dimensional  $XY$  model with the magnetic field in the time-direction; this allows the analogy to bulk superconductors, revealing the nature of the phase transitions.

PACS numbers: 74.50.+r, 67.40.Db

## I. INTRODUCTION

Two-dimensional (2D) superconducting arrays with charging effects have drawn much interest because of their interesting phase transitions [1] and relations to other systems such as the Bose-Hubbard model and the quantum  $XXZ$  spin model [2]. In those arrays where both the self-capacitance  $C_0$  and the junction capacitance  $C_1$  are present, charging energies due to both capacitances need to be considered simultaneously since the nature of the phase transition in general depends on them. For example, at zero temperature the system with only self-capacitance can be mapped into a classical three-dimensional (3D)  $XY$  model with the ratio  $E_0/E_J$  of the charging energy  $E_0 \equiv e^2/2C_0$  to the Josephson coupling strength  $E_J$  taking the role of the temperature. In the opposite limit, on the other hand, it is well known that there exists an interesting duality between charges and vortices [3,4], and the system with only junction capacitance at zero temperature undergoes a charge-unbinding Berezinskii-Kosterlitz-Thouless (BKT) transition [5] from the insulating phase to the superconducting one as the ratio  $E_J/E_1$  with  $E_1 \equiv e^2/2C_1$  is increased. The critical value  $(E_J/E_1)_c$ , beyond which the array is superconducting, has been found 0.6 in experiment [6], 0.23 in the duality argument [4] and in the variational method [7], 0.51 in perturbation expansion [8], and 0.36 in quantum Monte Carlo simulations [9]. As  $C_0$  is increased from zero in this system, the interactions between charges are screened, with the screening length given by  $\Lambda \equiv \sqrt{C_1/C_0}$  [4], and the nature of the phase transition is expected to alter. Recently, the zero-temperature phase diagrams have been studied by means of the perturbation expansion [8], which suggests that the phase transition from the Mott insulating phase to the superconducting phase is governed by the single-charge (SC) excitations or by the charge-dipole (CD) excitations, depending on

the ratio  $C_1/C_0$  as well as on the charge frustration.

In this paper, we study the quantum phase transitions in 2D superconducting arrays, focusing on the effects of external magnetic fields as well as the competition between self- and junction capacitances. The effects of external magnetic fields on phase transitions have been studied both in the classical arrays without charging energy [1] and in the quantum arrays [9–12]. However, most existing analytical works on the latter have employed mean-field-like approximations, which are not reliable in two dimensions. We thus adopt the perturbative expansion instead, and consider the SC and the CD excitations to the second order in  $E_J$ . The obtained phase boundaries between the Mott insulating phase and the superconducting one exhibit strong commensurability effects due to the magnetic frustration. The results are compared with experiments, suggesting the possibility that the experimentally observed transition may not be of the charge-unbinding BKT type. It is also shown that the dual transformation maps the system with both magnetic frustration and general capacitance onto a classical 3D  $XY$  model under the magnetic field in the time-direction. This transformation allows us to discuss the nature of the phase transitions, by analogy with bulk superconductors under magnetic fields.

There are four sections in this paper: Section II is devoted to the perturbative approach, from which the zero-temperature diagrams are obtained. We compare the phase diagrams with those obtained from the mean-field approach and those observed in experiments. In Sec. III the system is transformed into a classical 3D  $XY$  model under the magnetic field in the (imaginary) time direction. The nature of the phase transitions is discussed by analogy with bulk superconductors under magnetic fields. Finally, Sec. IV summarizes the results and presents some discussions.

## II. PERTURBATIVE APPROACH

We begin with the Hamiltonian describing the superconducting array with magnetic frustration:

$$H = 4E_0 \sum_{i,j} q_i \tilde{C}_{ij}^{-1} q_j - E_J \sum_{\langle i,j \rangle} \cos(\phi_i - \phi_j - A_{ij}) \quad (1)$$

$$\equiv H_0 + V,$$

---


$$\tilde{C}_{ij} \equiv (1 + 4C_1/C_0)\delta_{i,j} - (C_1/C_0)(\delta_{i,j+\hat{x}} + \delta_{i,j-\hat{x}} + \delta_{i,j+\hat{y}} + \delta_{i,j-\hat{y}}) \quad (2)$$


---

with the self-capacitance  $C_0$  and the junction capacitance  $C_1$ . The important external parameters  $E_0 \equiv e^2/C_0$  and  $E_J$  measure the self-charging energy and the Josephson coupling energy, respectively. The magnetic bond angle  $A_{ij}$  between the two sites  $i$  and  $j$  is given by the line integral of the magnetic vector potential  $\mathbf{A}$ :  $A_{ij} \equiv (2\pi/\Phi_0) \int_i^j \mathbf{A} \cdot d\mathbf{l}$  with the magnetic flux quantum  $\Phi_0 \equiv hc/2e$ .

When  $E_J = 0$ , the system described by the unperturbed Hamiltonian  $H_0$  has the Mott insulating phase as the ground state with the charge configuration  $q_i = 0$  at any site. In the opposite limit of  $E_0 = 0$ , on the other hand, the system is described by the 2D classical  $XY$  model, displaying superconductivity at zero temperature. It is thus expected that there exists a critical value of  $E_J/E_0$  beyond which the superconducting phase becomes energetically favorable. The critical value may be determined by comparing the energy of the Mott insulating phase with that of the superconducting phase. The energy  $E_M$  of the Mott insulating phase is easily computed up to the second order in  $E_J/E_0$ :

$$E_M = -\frac{E_J^2 N}{8E_0(\tilde{C}_{00}^{-1} - \tilde{C}_{\hat{x},0}^{-1})} \quad (3)$$

for the  $L \times L$  square array ( $N \equiv L^2$ ) (see Ref. [8] for the detailed calculation). It is of interest to note here that

---


$$P_{ij} \equiv \begin{cases} \exp(-iA_{ij}) & \text{for nearest neighboring sites } i \text{ and } j, \\ 0 & \text{otherwise.} \end{cases}$$


---

In the presence of the external magnetic field, the gauge-invariant magnetic frustration is defined by  $f \equiv \Phi/\Phi_0$  with  $\Phi$  being the magnetic flux per plaquette. If  $f = p/q$  with  $p$  and  $q$  being relative primes, it is obvious that  $P_{ij}$  is invariant under the magnetic translation of  $q$  lattice sites. Noting this translational symmetry, we represent the position of site  $i$  by the vector  $\mathbf{R}+\mathbf{a}$ , where  $\mathbf{R}$  is the

where the charge  $q_j$  at site  $j$  represented in units of  $2e$  ( $e > 0$ ) and the phase  $\phi_k$  of the superconducting order parameter at site  $k$  satisfy the commutation relation  $[\phi_k, q_j] = i\delta_{jk}$ . Whereas the summation in the second term runs over all nearest neighboring pairs, the charges interact via the inverse of the dimensionless capacitance matrix  $\tilde{C}_{ij}$  defined by

$E_M$  does not depend on the external magnetic field.

Since the lowest excitation that can lead to the change of the ground state from the Mott insulating into the superconducting phase is presumably point-like, and we consider two kinds of excitations: the SC and the CD excitations. We first consider the SC-type excited state and write its energy up to the second order in  $E_J/E_0$ :

$$E_{SC} = E_{SC}^{(0)} + E_{SC}^{(1)} + E_{SC}^{(2)}. \quad (4)$$

In the SC-type excited state a single positive charge is located only at one site, and the zeroth-order energy is given by

$$E_{SC}^{(0)} = 4E_0 \sum_{i,j} q_i \tilde{C}_{ij}^{-1} q_j = 4E_0 \tilde{C}_{00}^{-1}. \quad (5)$$

Since the single charge can be located at any site without any energy difference, we need to make use of the degenerate perturbation theory. In the first order it is thus necessary to diagonalize the matrix

$$\langle i|V|j \rangle = -\langle i|E_J \sum_{\langle k,l \rangle} \cos(\phi_k - \phi_l - A_{kl})|j \rangle \equiv -\frac{E_J}{2} P_{ij}, \quad (6)$$

where  $|i \rangle$  denotes the charge eigenstate with the single charge at site  $i$  and the matrix element  $P_{ij}$  is defined by

---

position vector of the  $q \times q$  superlattice unit cell containing site  $i$  and  $\mathbf{a}$  denotes the relative position of site  $i$  inside the superlattice (see Fig. 1), and write

$$P_{ij} = P(\mathbf{R}, \mathbf{a}; \mathbf{R}', \mathbf{a}') = P(\mathbf{R}-\mathbf{R}', \mathbf{a}; \mathbf{0}, \mathbf{a}'). \quad (7)$$

Through the Fourier transformation

$$\begin{aligned}\bar{v}^{(\mathbf{p})}(\mathbf{a}) &\equiv \frac{1}{\sqrt{M}} \sum_{\mathbf{R}} e^{i\mathbf{p}\cdot\mathbf{R}} v(\mathbf{R}+\mathbf{a}), \\ \bar{P}^{(\mathbf{p})}(\mathbf{a}; \mathbf{a}') &\equiv \sum_{\mathbf{R}} e^{i\mathbf{p}\cdot\mathbf{R}} P(\mathbf{R}, \mathbf{a}; \mathbf{0}, \mathbf{a}'),\end{aligned}\quad (8)$$

the matrix is block-diagonalized, resulting in the eigenvalue equations

$$\sum_{\mathbf{a}'} \bar{P}^{(\mathbf{p})}(\mathbf{a}; \mathbf{a}') \bar{v}^{(\mathbf{p})}(\mathbf{a}') = \lambda^{(\mathbf{p})} \bar{v}^{(\mathbf{p})}(\mathbf{a}), \quad (9)$$

where  $M \equiv N/q^2$  is the total number of superlattices, and  $v(\mathbf{R}+\mathbf{a}) \equiv v_i$  is the wavefunction for the eigenstate of  $P_{ij}$ . The numerical diagonalization of  $M$  Hermitian matrices  $\bar{P}^{(\mathbf{p})}(\mathbf{a}; \mathbf{a}')$ , each of the size  $q^2 \times q^2$ , yields the largest eigenvalue  $P_{\max}$ , which in turn gives the first-order energy

$$E_{\text{SC}}^{(1)} = -E_J P_{\max}/2. \quad (10)$$

It is well known that the largest eigenvalue  $P_{\max}$  always shows up for  $\mathbf{p} = 0$ , and further, the eigenstates corresponding to the eigenvalue  $P_{\max}$  are  $q$ -fold degenerate for  $f = p/q$  [13]. Since the degeneracy is not completely removed in the first-order calculation, it is necessary to diagonalize the second-order matrix  $Q$  with the element given by

$$Q_{dd'} = \sum_{\mathbf{q} \notin D} \frac{\langle d|V|\mathbf{q}\rangle \langle \mathbf{q}|V|d'\rangle}{E_{\text{SC}}^{(0)} - E_{\mathbf{q}}^{(0)}}, \quad (11)$$

where the summation runs over all the charge eigenstates  $|\mathbf{q}\rangle$  outside the space  $D$  spanned by the SC states, and  $|d\rangle$  represents the  $d$ th eigenstate corresponding to the eigenvalue  $P_{\max}$ :

$$|d\rangle = \sum_i v_{d,i} |i\rangle = \sum_{\mathbf{R}, \mathbf{a}} v_d(\mathbf{R}+\mathbf{a}) |\mathbf{R}+\mathbf{a}\rangle. \quad (12)$$

Here the wavefunction  $v_d(\mathbf{R}+\mathbf{a})$  of the  $d$ th degenerate state is related to the component  $\bar{v}_d(\mathbf{a})$  of the normalized eigenvector of  $\bar{P}$  via

$$v_d(\mathbf{R}+\mathbf{a}) = \frac{1}{\sqrt{M}} \bar{v}_d(\mathbf{a}), \quad (13)$$

where the superscript in  $\bar{v}_d^{\mathbf{p}=0}(\mathbf{a})$  has been omitted for simplicity [see Eq. (8)]. Inserting Eqs. (12) and (13) into Eq. (11), we obtain

$$Q_{dd'} = \sum_{\mathbf{R}} \sum_{\mathbf{a}, \mathbf{a}'} \bar{v}_d^*(\mathbf{a}) \bar{v}_{d'}(\mathbf{a}') \tilde{Q}_{\mathbf{R}+\mathbf{a}, \mathbf{a}'} \quad (14)$$

with

$$\tilde{Q}_{\mathbf{R}+\mathbf{a}, \mathbf{a}'} \equiv \sum_{\mathbf{q} \notin D} \frac{\langle i|V|\mathbf{q}\rangle \langle \mathbf{q}|V|j\rangle}{E_{\text{SC}}^{(0)} - E_{\mathbf{q}}^{(0)}} \equiv \tilde{Q}_{ij}.$$

It is obvious that  $\tilde{Q}_{ij}$  does not vanish only when  $|i\rangle$  and  $|j\rangle$  are related by two successive charge hoppings as shown in Fig. 2. When  $i = j$  (denoted by an empty circle in Fig. 2), it is easy to find that

$$\tilde{Q}_{ii} = \frac{E_J^2}{32E_0} \sum'_{(m,n)} \frac{1}{(\tilde{C}_{ni}^{-1} - \tilde{C}_{mi}^{-1}) - (\tilde{C}_{00}^{-1} - \tilde{C}_{\mathbf{x},0}^{-1})}, \quad (15)$$

where the summation  $\sum'_{(m,n)}$  runs over  $m$  and its four nearest neighbors  $n$  with the restriction of nonzero denominator. When  $j = i \pm \hat{\mathbf{x}} \pm \hat{\mathbf{y}}$  (denoted by 'x' symbols in Fig. 2), there exist two intervening states  $|\mathbf{q}\rangle$ , yielding

$$\tilde{Q}_{i,j=i\pm\hat{\mathbf{x}}\pm\hat{\mathbf{y}}} = \frac{E_J^2}{32E_0} \frac{e^{i(A_j, i\pm\hat{\mathbf{x}}+A_{i\pm\hat{\mathbf{x}},i})} + e^{i(A_j, i\pm\hat{\mathbf{y}}+A_{i\pm\hat{\mathbf{y}},i})}}{(\tilde{C}_{\mathbf{x},0}^{-1} - \tilde{C}_{\mathbf{x}\pm\hat{\mathbf{y}},0}^{-1}) - (\tilde{C}_{00}^{-1} - \tilde{C}_{\mathbf{x},0}^{-1})}. \quad (16)$$

On the other hand, when  $j = i \pm 2\hat{\mathbf{x}}(2\hat{\mathbf{y}})$  as represented by filled circles in Fig. 2, the matrix element is computed to be

$$\tilde{Q}_{i,j=i\pm 2\hat{\mathbf{x}}(2\hat{\mathbf{y}})} = \frac{E_J^2}{32E_0} \frac{e^{i(A_j, i\pm\hat{\mathbf{x}}(\hat{\mathbf{y}})+A_{i\pm\hat{\mathbf{x}}(\hat{\mathbf{y}},i)})}}{(\tilde{C}_{\mathbf{x},0}^{-1} - \tilde{C}_{2\hat{\mathbf{x}},0}^{-1}) - (\tilde{C}_{00}^{-1} - \tilde{C}_{\mathbf{x},0}^{-1})}. \quad (17)$$

Equations (15) – (17) together with the eigenvector  $\bar{v}$  obtained in the first-order calculation yield the explicit form of the matrix element  $Q_{dd'}$  in Eq. (14). The matrix  $Q$  is then diagonalized to give the minimum eigenvalue  $Q_{\min}$ , which in turn leads to the energy of the SC state:

$$E_{\text{SC}} = E_{\text{SC}}^{(0)} + E_{\text{SC}}^{(1)} + E_{\text{SC}}^{(2)} = 4E_0 \tilde{C}_{00}^{-1} - E_J P_{\max}/2 + Q_{\min}. \quad (18)$$

Comparing it with the energy of the Mott phase in Eq. (3), we find the phase boundary between the Mott insulating phase and the superconducting phase. Figure 3 shows the obtained phase boundaries separating the superconducting phase (above each curve) and the

insulating one (below) on the plane of  $E_J/E_0$  and  $f$ , for various values of  $C_1/C_0$ . In obtaining the critical values  $(E_J/E_0)_c$  numerically, we have considered systems of sufficiently large sizes, so that the critical values display convergence in at least three significant digits, for given

parameters  $f$  and  $C_1/C_0$ . Thus the system size has been increased up to  $N = 384$ , depending on the values of  $f$  and  $C_1/C_0$ , and the convergence has been confirmed.

It is obvious that the superconducting region expands as the junction capacitance  $C_1$  is increased, confirming the results in Refs. [7,8]. In particular, the obtained phase diagrams are entirely similar to those obtained for  $C_0 \gg C_1$  in the mean-field approximation [12], demonstrating significant commensurate-incommensurate effects due to the magnetic frustration. Quantitatively, however, there exists discrepancy between the results of the perturbation expansion and those from the mean-field approaches: The estimated critical values in the former are rather larger. Furthermore, the perturbation expansion yields the ratio of the critical value for  $f = 1/2$  to that for  $f = 0$  approximately given by 1.9 for  $C_1/C_0 \lesssim 0.1$  (see Fig. 3); this is larger than the value  $\sqrt{2}$  predicted in the self-charging limit within the mean-field approximation [11,12]. The increase of  $C_1/C_0$  is found to reduce the ratio monotonically. It is of interest to notice here that the first-order calculation reproduces the mean-field value  $\sqrt{2}$  regardless of  $C_1/C_0$ .

We now consider the CD-type excited state, where there exists a pair of positive and negative charges separated by the lattice spacing. The energy of the CD state

is written as

$$E_{\text{CD}} = E_{\text{CD}}^{(0)} + E_{\text{CD}}^{(1)} + E_{\text{CD}}^{(2)} \quad (19)$$

up to the second order in  $E_J/E_0$ . The zeroth- and the first-order energies are easily calculated:  $E_{\text{CD}}^{(0)} = 8E_0(\tilde{C}_{00}^{-1} - \tilde{C}_{\hat{x},0}^{-1})$  and  $E_{\text{CD}}^{(1)} = 0$ . To calculate the second-order term, we apply the second-order degenerate perturbation theory, and diagonalize the matrix  $M$ , the element of which is given by

$$\langle i, j | M | k, l \rangle \equiv \sum_{\mathbf{q} \notin D} \frac{\langle i, j | V | \mathbf{q} \rangle \langle \mathbf{q} | V | k, l \rangle}{E_{\text{CD}}^{(0)} - E_{\mathbf{q}}^{(0)}}. \quad (20)$$

Here  $|k, l\rangle$  is the CD states with the positive charge at site  $k$  and the negative charge at site  $l$ , where  $l$  is one of the four nearest neighbors of  $k$ , and the sum is performed over the intervening states  $|\mathbf{q}\rangle$  outside the space  $D$  spanned by all CD states. The above matrix element does not vanish only when  $|k, l\rangle$  can be connected to  $|i, j\rangle$  by two successive charge hoppings. Figure 4 shows all possible states of  $|k, l\rangle$  when  $|i, j\rangle$  is given as in Fig. 4(a). While the matrix element corresponding to Fig. 4(a) is given by

$$\langle i, j | M | i, j \rangle = \frac{E_J^2}{32E_0} \sum'_{(k,l)} \frac{1}{(\tilde{C}_{li}^{-1} - \tilde{C}_{ki}^{-1}) - (\tilde{C}_{lj}^{-1} - \tilde{C}_{kj}^{-1}) - (\tilde{C}_{00}^{-1} - \tilde{C}_{\hat{x},0}^{-1})}, \quad (21)$$

there is only one intervening state in the case of Fig. 4(b), leading to

$$\langle i, j | M | j, i \rangle = \frac{E_J^2}{32E_0} \frac{e^{2iA_{ji}}}{\tilde{C}_{00}^{-1} - \tilde{C}_{\hat{x},0}^{-1}}. \quad (22)$$

For  $|k, l\rangle$  given by the state in Figs. 4(c) and (d), we find

$$\langle i, j | M | i, l=i_\alpha \rangle = \frac{E_J^2}{32E_0} \left[ \frac{e^{i(A_{j,i} + A_{i,l})}}{\tilde{C}_{00}^{-1} - \tilde{C}_{\hat{x},0}^{-1}} + \frac{e^{i(A_{j,j_\alpha} + A_{j_\alpha,l})}}{\tilde{C}_{\hat{x}+\hat{y},0}^{-1} - \tilde{C}_{\hat{x},0}^{-1}} + \frac{e^{i(A_{j_\alpha,l} + A_{j,j_\alpha})}}{3\tilde{C}_{\hat{x},0}^{-1} - 2\tilde{C}_{\hat{x}+\hat{y},0}^{-1} - \tilde{C}_{00}^{-1}} \right. \\ \left. + \frac{e^{i(A_{i,l} + A_{j,i})}}{3\tilde{C}_{\hat{x},0}^{-1} - \tilde{C}_{\hat{x}+\hat{y},0}^{-1} - 2\tilde{C}_{00}^{-1}} \right], \quad (23)$$

where  $i_\alpha$  denotes the  $\alpha$ th nearest neighboring site of  $i$  ( $\alpha = 1, 2, 3, 4$ ). Similarly, we get

$$\langle i, j | M | k=j_\alpha, j \rangle = \frac{E_J^2}{32E_0} \left[ \frac{e^{i(A_{j,i} + A_{k,j})}}{\tilde{C}_{00}^{-1} - \tilde{C}_{\hat{x},0}^{-1}} + \frac{e^{i(A_{i_\alpha,i} + A_{k,i_\alpha})}}{\tilde{C}_{\hat{x}+\hat{y},0}^{-1} - \tilde{C}_{\hat{x},0}^{-1}} + \frac{e^{i(A_{k,i_\alpha} + A_{i_\alpha,i})}}{3\tilde{C}_{\hat{x},0}^{-1} - 2\tilde{C}_{\hat{x}+\hat{y},0}^{-1} - \tilde{C}_{00}^{-1}} \right. \\ \left. + \frac{e^{i(A_{k,j} + A_{j,i})}}{3\tilde{C}_{\hat{x},0}^{-1} - \tilde{C}_{\hat{x}+\hat{y},0}^{-1} - 2\tilde{C}_{00}^{-1}} \right] \quad (24)$$

for Figs. 4(e) and (f),

$$\langle i, j | M | k, l \rangle = \frac{E_J^2}{32E_0} \left[ \frac{e^{i(A_{j,i} + A_{k,l})}}{\tilde{C}_{00}^{-1} - \tilde{C}_{\hat{x},0}^{-1}} + \frac{e^{2i(A_{k,i} + A_{j,l})}}{\tilde{C}_{\hat{x}+\hat{y},0}^{-1} - \tilde{C}_{\hat{x},0}^{-1}} + \frac{e^{i(A_{k,l} + A_{j,i})}}{2\tilde{C}_{\hat{x}+\hat{y},0}^{-1} - 3\tilde{C}_{\hat{x},0}^{-1} - \tilde{C}_{00}^{-1}} \right] \quad (25)$$

for Figs. 4(g) and (h), and finally

$$\langle i, j | M | k, l \rangle = \frac{E_J^2}{32E_0} \left[ \frac{e^{i(A_{j,i} + A_{k,i})}}{\tilde{C}_{00}^{-1} - \tilde{C}_{\hat{x},0}^{-1}} + \frac{e^{i(A_{j,i} + A_{k,l})}}{(\tilde{C}_{li}^{-1} - \tilde{C}_{ki}^{-1}) - (\tilde{C}_{lj}^{-1} - \tilde{C}_{kj}^{-1}) - (\tilde{C}_{00}^{-1} - \tilde{C}_{\hat{x},0}^{-1})} \right] \quad (26)$$

for the cases corresponding to Fig. 4(i). Equations (21)–(26) give the  $4N \times 4N$  matrix  $M$ , which, again via the Fourier transformation, reduces to  $4q^2 \times 4q^2$  Hermitian matrices for  $f = p/q$ . By diagonalizing numerically the resulting matrices, we obtain the second-order energy  $E_{\text{CD}}^{(2)}$ , the comparison of which with the energy of the Mott insulating phase given by Eq. (3) yields the phase boundaries. Figure 5 displays the obtained boundaries in the plane of  $E_J/E_1$  and  $f$ . As in obtaining Fig. 3, we have considered systems of such large sizes that at least three significant digits of the critical values  $(E_J/E_1)_c$  are obtained for given values of  $f$  and  $C_1/C_0$ .

In experiment on the arrays with  $C_1/C_0 \approx 100$ , the critical values  $(E_J/E_1)_c \approx 0.6$  for  $f = 0$  and  $0.9$  for  $f = 1/2$  have been observed [6]; this is to be compared with the corresponding values obtained in the perturbation scheme here, with the CD excitations taken into consideration:  $(E_J/E_1)_c \approx 0.503$  for  $f = 0$  and  $0.508$  for  $f = 1/2$ . Remarkably, the consideration of CD excitations yields the critical value for  $f = 1/2$  not far larger than that for  $f = 0$ , in disagreement with the experimental result. On the other hand, the phase boundary computed from the consideration of the SC excitations for  $C_1/C_0 = 100$ , shown in Fig. 6, is in general consistent with that measured in experiment [6]. Contrary to the usual anticipation that CD excitations play a crucial role in destroying the Mott insulating phase for  $C_1 \gg C_0$ , this apparently suggests that the superconductor-insulator transition observed in experiment is driven by SC excitations rather than by CD ones, raising the interesting possibility that the transition may not be of the BKT

type.

### III. DUAL TRANSFORMATION APPROACH

In this section, we examine the nature of the phase transitions discussed above in terms of the topological excitations. This is achieved by means of the mapping of the quantum phase model given by Eq. (1) into an effective 3D classical model; this approach was already adopted by other authors in the absence of the external magnetic field [4]. We begin with the Euclidean action, corresponding to the Hamiltonian in Eq. (1), in the imaginary-time path-integral representation:

$$S = +i \sum_{j,\tau} q_{j,\tau} \nabla_\tau \phi_{j,\tau} + \frac{1}{2K} \sum_{ij,\tau} q_{i,\tau} C_{ij}^{-1} q_{j,\tau} - K \sum_{j,\mu,\tau} \cos[\nabla_\mu \phi_{j,\tau} - 2\pi A_{\mu;j}], \quad (27)$$

where  $K \equiv \sqrt{E_J/8E_0}$ ,  $A_{\mu;j} \equiv A_{j,j+\hat{\mu}}$ ,  $\nabla_\mu$  ( $\mu = x, y$ ) and  $\nabla_\tau$  are difference operators in the space and time directions, respectively, and the (imaginary) time-slice spacing  $\delta\tau$  has been chosen to be  $\sqrt{8E_J E_0}/\hbar$  [14]. In the nearest-neighbor charging limit ( $C_0 = 0$ ), the coupling constant and the time-slice spacing in Eq. (27) are given by  $K \equiv \sqrt{E_J/8E_1}$  and  $\delta\tau = \sqrt{8E_J E_1}/\hbar$ , respectively. Standard procedures [15,16] then lead to the dual form of Eq. (27), which is simply the effective Hamiltonian for the 3D classical system of vortex loops:

$$H_V = -\pi K \sum_{i,j,\tau,\tau'} \sum_{\mu=x,y,\tau} [v_\mu(\mathbf{r}_i, \tau) - \delta_{\mu,\tau} f] \hat{U}_\mu(\mathbf{r}_i - \mathbf{r}_j, \tau - \tau') [v_\mu(\mathbf{r}_j, \tau') - \delta_{\mu,\tau} f]. \quad (28)$$

Here the vortex interaction  $\hat{U}_\mu(\mathbf{r}, \tau) \equiv 2\pi [U_\mu(0, 0) - U_\mu(\mathbf{r}, \tau)]$  is determined by the Fourier transforms

$$\tilde{U}_x(\mathbf{q}, \omega) = \tilde{U}_y(\mathbf{q}, \omega) = \frac{\tilde{C}(\mathbf{q})}{\Delta(q_x) + \Delta(q_y) + \tilde{C}(\mathbf{q})\Delta(\omega)} \quad (29)$$

$$\tilde{U}_\tau(\mathbf{q}, \omega) = \frac{1}{\Delta(q_x) + \Delta(q_y) + \tilde{C}(\mathbf{q})\Delta(\omega)} \quad (30)$$

with  $\Delta(q) \equiv 2(1 - \cos q)$ . The Fourier transform of the capacitance matrix is given by  $\tilde{C}(\mathbf{q}) = 1 + (C_1/C_0)[\Delta(q_x) + \Delta(q_y)]$  for  $C_0 \neq 0$  and  $\tilde{C}(\mathbf{q}) = \Delta(q_x) + \Delta(q_y)$  for  $C_0 = 0$ .

Note also that the vortex lines can terminate nowhere but form closed loops or go to infinity, as implied by the condition  $\nabla \cdot \mathbf{v}(\mathbf{r}, \tau) = 0$ .

The behavior of the interaction  $\hat{U}_\mu(\mathbf{r}, \tau)$  in Eq. (28) depends crucially on whether  $C_0$  vanishes, since the Coulomb interaction between charges (Cooper pairs) is infinitely long-ranged for  $C_0 = 0$ . If  $C_0 \neq 0$ , one can show, in the same manner as in Ref. [16], that at large scales ( $\sqrt{r^2 + \tau^2} \gg 1$ ) the interaction  $\hat{U}_\mu$  is isotropic and displays the asymptotic behavior  $\hat{U}_\mu(\mathbf{r}, \tau) \sim -1/\sqrt{r^2 + \tau^2}$  apart from an additive constant, regardless of the ratio  $C_1/C_0$ . Accordingly, the system is described by the 3D isotropic  $XY$  model under an external magnetic field in the  $\tau$ -direction, the topological representation of which is given by Eq. (28). The 3D  $XY$  model has been widely used as a model for the bulk superconductor at temperatures low enough to neglect the amplitude fluctuations of the order parameter [17]. By analogy with the vortex lattice melting transition at the temperature  $T_m(H)$  in the mixed state of a type-II superconductor, a first-order phase transition is expected at  $K_c(f)$  in our system under the magnetic field, as  $K$  is increased from zero [17,18]. At zero field, in particular, the phase transition should be continuous, belonging to the 3D  $XY$  universality class [4].

For  $C_0 = 0$ , on the other hand, the interaction is highly anisotropic:  $\hat{U}_x(\mathbf{r}, \tau) = \hat{U}_y(\mathbf{r}, \tau) \sim \exp(-\sqrt{r^2 + \tau^2})$  while  $\hat{U}_\tau(\mathbf{r}, \tau) \sim e^{-|\tau|} \log r$ . Thus the equivalent classical system described by Eq. (28) forms a layered structure of planar spins with strongly anisotropic coupling constants. The 3D anisotropic  $XY$  model has also been studied extensively as a special case of the Lawrence-Doniach model for high-temperature superconductors [17,19]: The effectively low dimensionality enhances the phase fluctuations and lowers the transition point  $K_c(f)$  [17]. Furthermore, at zero field, the strong anisotropy drives the transition to be of the BKT type [4,19].

These arguments have been summarized in Fig. 7. Note that the important effects of frustration arising from the commensurability between the flux lattice and the underlying lattice are disregarded here. Such continuum approximation is believed to be qualitatively valid in low field regions (represented by the solid lines in Fig. 7). As the field is increased, frustration effects are expected to come into play and to yield sensitive dependence of the transition on the field, reproducing the perturbative results shown in Figs. 3 and 5.

#### IV. CONCLUSION

We have studied the zero-temperature phase transitions of two-dimensional superconducting arrays with both self- and junction capacitances in the presence of external magnetic fields. Through the use of the second-order perturbation theory, we have considered both single-charge excitations and charge-dipole excitations, from which the phase diagrams are obtained. It has been found that the phase boundaries are quite sensitive to the variation of the magnetic frustration due to

the commensurate-incommensurate effects. In particular, the superconductor-insulator transition observed in experiment has been suggested to be driven by single-charge excitations rather than by charge-dipole ones, and thus the possibility that the transition may not be of the Berezinskii-Kosterlitz-Thouless type has been pointed out. In this regard, it is noteworthy that the lowest excitation has already been shown to be comprised by the single-charge type rather than the charge-dipole type even for large values of  $C_1/C_0$ , so long as there exists finite charge frustration [8]. In experiment, it is practically impossible to set the charge frustration exactly zero, and accordingly, the lowest excitation should presumably be of the single-charge type even in the nearest-neighbor charging limit. Indeed it has recently been pointed out that the absence of the Berezinskii-Kosterlitz-Thouless charge-unbinding transition in experiments [6] may be attributed to the presence of the finite charge frustration which is randomly distributed over the arrays [20].

We have also transformed the system to a 3D classical  $XY$  model under magnetic fields in the time direction. The nature of the phase transitions at low magnetic fields has been discussed, based on the analogy with the bulk superconductor under magnetic fields. Unfortunately, unlike in the 2D  $XY$  model, there have been few studies of the frustration effects in the 3D  $XY$  model, which disallows quantitative comparison at this stage. Nevertheless, the analogy with the continuum superconductor provides a complement to the perturbative estimate of the phase boundaries, already giving a clue to the nature of the phase transitions.

#### ACKNOWLEDGMENTS

This work was supported in part by the Basic Science Research Institute Program, Ministry of Education, in part by the Korea Science and Engineering Foundation through the SRC Program. MSC was also supported in part by the Ministry of Science and Technology through the Creative Research Initiative Program.

- 
- \* Present address: Department of Theoretical Physics, Umeå University, S-901 87 Umeå, Sweden
- [1] For a list of references, see, e.g., *Proceedings of the 2nd CTP workshop on Statistical Physics: KT Transition and Superconducting Arrays*, edited by D. Kim, J.S. Chung, and M.Y. Choi (Min-Eum Sa, Seoul, 1993); *Physica B* **222** 253-406 (1996).
  - [2] A. van Otterlo, K.-H. Wagenblast, R. Baltin, C. Bruder, R. Fazio, and G. Schön, *Phys. Rev. B* **52**, 16 176 (1995).
  - [3] L.V. Keldysh, *Pis'ma Zh. Eksp. Teor. Fiz.* **29**, 716 (1979) [*JETP Lett.* **29**, 658 (1979)]; J.E. Mooij, B.J. van Wees,

- L.J. Geerligs, M. Peters, R. Fazio, and G. Schön, Phys. Rev. Lett. **65**, 645 (1990).
- [4] R. Fazio and G. Schön, Phys. Rev. B **43**, 5307 (1991), and references therein.
- [5] V.L. Berezinskii, Zh. Eksp. Teor. Fiz. **59**, 907 (1970) [Sov. Phys. JETP **32**, 493 (1971)]; J.M. Kosterlitz and D.J. Thouless, J. Phys. C **6**, 1181 (1973); J.M. Kosterlitz, *ibid.* **7**, 1046 (1974); J.V. José, L.P. Kadanoff, S. Kirkpatrick, and D.R. Nelson, Phys. Rev. B **16**, 1217 (1977).
- [6] H.S.J. van der Zant, L.J. Geerligs, and J.E. Mooij, Europhys. Lett. **19**, 541 (1992); H.S.J. van der Zant, W.J. Elion, L.J. Geerligs, and J.E. Mooij, Phys. Rev. B **54**, 10 081 (1996).
- [7] B.J. Kim and M.Y. Choi, Phys. Rev. B **52**, 3624 (1995).
- [8] B.J. Kim, J. Kim, S.Y. Park, and M.Y. Choi, Phys. Rev. B **56**, 395 (1997).
- [9] C. Rojas and J.V. José, Phys. Rev. B **54**, 12 361 (1996).
- [10] A. Kampf and G. Schön, Phys. Rev. B **37**, 5954 (1988); A. van Otterlo, K.-H. Wagenblast, R. Fazio, and G. Schön, *ibid.* **48**, 3316 (1993).
- [11] E. Granato and J.M. Kosterlitz, Phys. Rev. Lett. **65**, 1267 (1990).
- [12] C. Bruder, R. Fazio, A. Kampf, A. van Otterlo, and G. Schön, Phys. Scr. T **42**, 159 (1992).
- [13] M.Y. Choi and S. Doniach, Phys. Rev. B **31**, 4516 (1985).
- [14] The critical behavior of the system should not be affected by the choice of  $\delta\tau$ ; see, e.g., S. L. Sondhi, S. M. Girvin, J. P. Carini and D. Shahar, Rev. Mod. Phys. **69**, 315 (1997). Here all the dynamics of the system occurs over the time scale  $\hbar/\sqrt{8E_J E_0}$  (or  $\hbar/\sqrt{8E_J E_1}$  for  $C_0 = 0$ ), making the choice proper.
- [15] R. Savit, Rev. Mod. Phys. **52**, 453 (1980); P.R. Thomas and M. Stone, Nucl. Phys. B **144**, 513 (1978).
- [16] M.-S. Choi, J. Yi, M.Y. Choi, J. Choi, and S.-I. Lee, Phys. Rev. B **57**, R716 (1998).
- [17] See, e.g., G. Blatter, M.V. Feigel'man, V.B. Geshkenbein, A.I. Larkin, and V.M. Vinokur, Rev. Mod. Phys. **66**, 1125 (1994), and references therein.
- [18] The upper critical field  $H_{c2}$  for a type-II superconductor is irrelevant in our consideration here; ideally, the system corresponds to the limit  $H_{c2} \rightarrow \infty$ .
- [19] S. E. Korshunov, Europhys. Lett. **11**, 757 (1990), and references therein.
- [20] P. Delsing, C.D. Chen, D.B. Haviland, T. Bergsten, and T. Claeson, *Lecture note in the Euroschool on Superconductivity in Network and Mesoscopic Structures* (unpublished); A.D Zaikin and S.V. Panyukov, Czech. J. Phys. **46**(S2), 629 (1996).

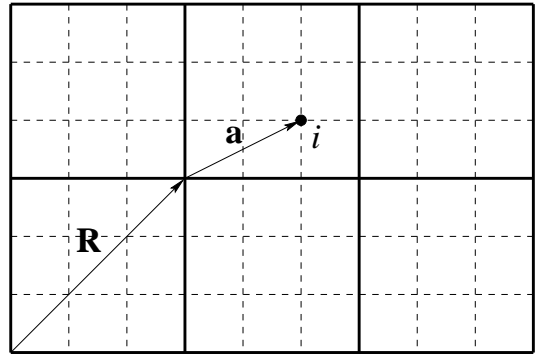


FIG. 1. Superconducting array of size  $9 \times 6$  with the magnetic frustration  $f = 1/3$ . The  $3 \times 3$  superlattices are indicated by thick solid lines. The position of the  $i$ th lattice site is represented by  $\mathbf{R} + \mathbf{a}$ , where  $\mathbf{R}$  and  $\mathbf{a}$  denote the position of the superlattice and the relative position of the site inside the superlattice, respectively.

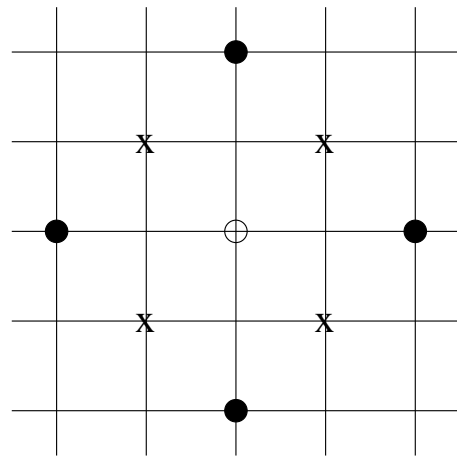


FIG. 2. Three cases in which the second-order matrix  $\tilde{Q}_{ij}$  has nonzero values. Only the single-charge states  $|j\rangle$  with  $j$  at positions marked by the empty circle, the filled circles, and the 'x' symbols, can be connected by two successive charge hoppings, to the state  $|i\rangle$  with  $i$  at the center (o).

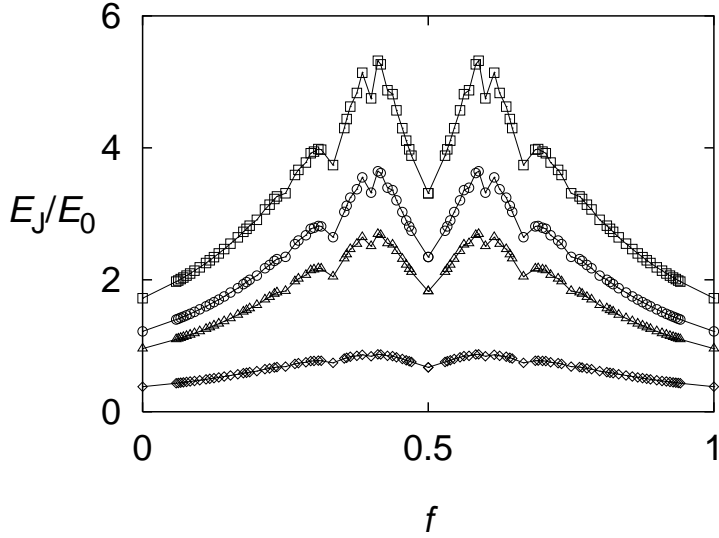


FIG. 3. Phase boundaries between the Mott insulating phase (below each curve) and the superconducting phase (above), computed from the consideration of single-charge excitations. Boundaries for various ratios of the junction capacitance  $C_1$  to the self-capacitance  $C_0$  are shown:  $C_1/C_0 = 0.0001(\square)$ ,  $0.1(\circ)$ ,  $0.2(\triangle)$ , and  $1.0(\diamond)$ . It is observed that the superconducting region expands as the junction capacitance is increased.

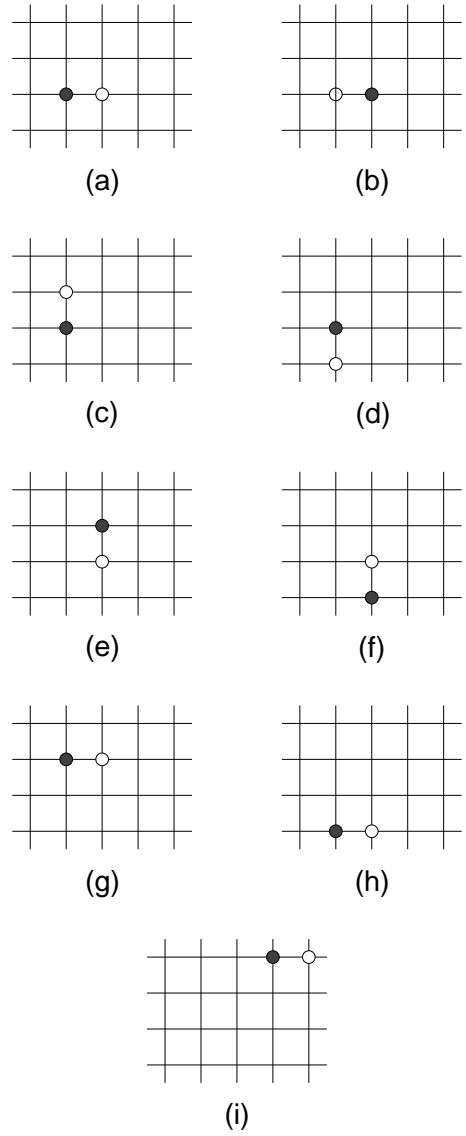


FIG. 4. The charge-dipole-type states  $|k, l\rangle$  giving nonzero elements of the second-order matrix  $\langle i, j|M|k, l\rangle$  in case that  $|i, j\rangle$  has the charge configuration of a positive charge at site  $i$  and a negative charge at  $j$  as shown in (a). The filled and the empty circles denote the positive and the negative charges, respectively. (i) shows an example of the states not included in (a)-(h).

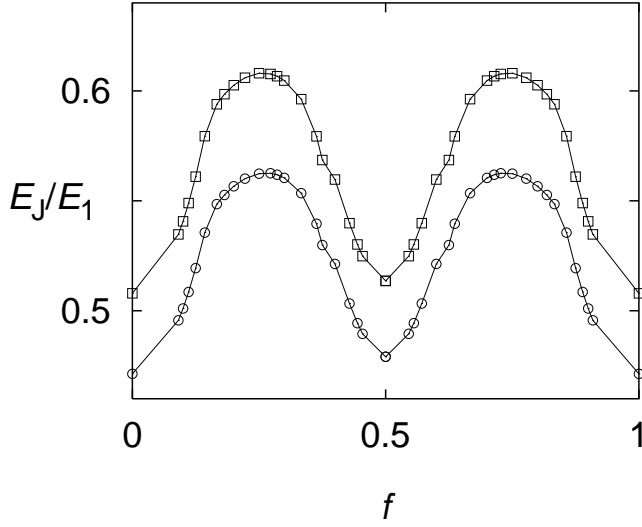


FIG. 5. Phase boundaries between the Mott insulating phase (below each curve) and the superconducting phase (above) of the charge-dipole type excitation. The upper curve is for  $C_1/C_0 = 10000$  while the lower one is for  $C_1/C_0 = 10$ .

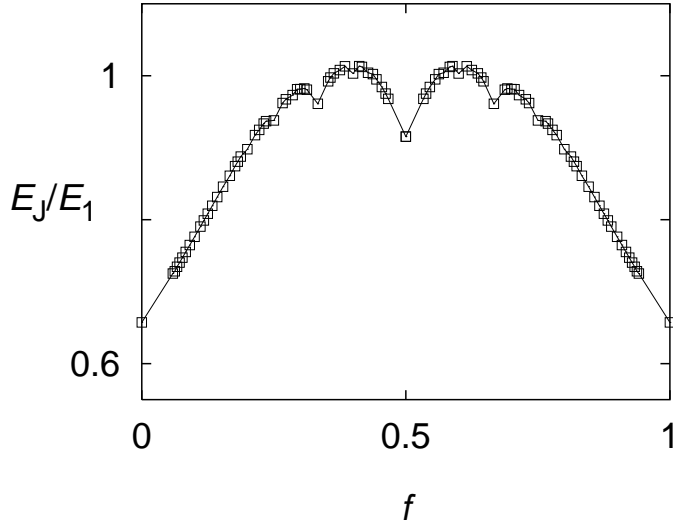
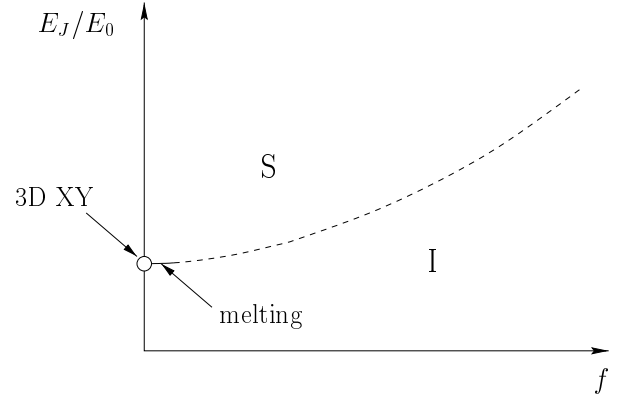
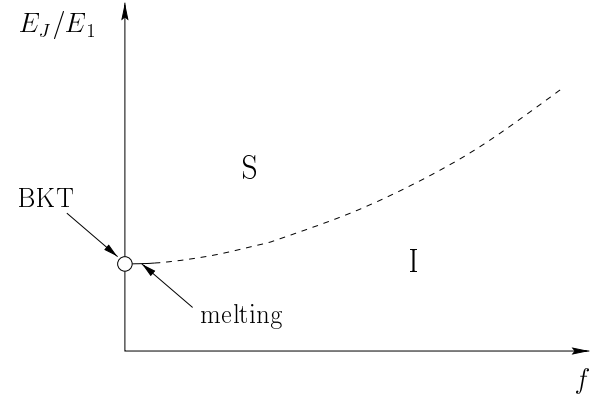


FIG. 6. Phase boundaries in the plane of  $E_J/E_1$  and  $f$  for  $C_1/C_0 = 100$  between the Mott insulating phase (below the curve) and the superconducting phase (above) computed from the consideration of single-charge excitations. The obtained critical values  $(E_J/E_1)_c \approx 0.657$  for  $f = 0$  and  $0.915$  for  $f = 1/2$  are in good agreement with the experimental results.



(a)



(b)

FIG. 7. Schematic diagram of the phase boundaries (a) for  $C_0 \neq 0$  and (b) for  $C_0 = 0$ . The dashed lines are valid only for continuum systems.